Transaction A: Civil Engineering
Vol. 17, No. 4, pp. 297–311

SCIENTIA IRANICA

Experimental and Numerical Investigations on Flooding System of Iranian South-Coast Dry Docks

A. Najafi-Jilani[1,*], M. Monshizadeh[2] and A. Naghavi[1]

Abstract. *Experimental investigations were carried out on the flooding system of the Bandar-Abbas dry dock, located on the southern coast of Iran. The main goal of the investigation was to evaluate the flooding time, as well as the seawater flow specifications, in the intake channels. The time variable upstream and downstream boundary conditions were simulated. The effects of tidal fluctuations on water discharge through the intake channels were inspected. The flow pattern around the bed overflow weirs of the intake channel was also investigated. The air trapping at the top of the main intake channel was recognized as an effective phenomenon on the flooding rate. A numerical model is simultaneously developed to evaluate the flow pattern and the velocity and pressure domain in the watering channels. Applicable guidance about selection of the element type and optimization of the convergence rate of the numerical modeling was presented especially for flow simulation under unsteady boundary conditions and complex geometry. Numerical results were compared with corresponding laboratory measured data and a good agreement was obtained.*

Keywords: *Graving dock; Flooding system; Tidal fluctuations; Numerical modeling; Experimental investigations.*

INTRODUCTION

Most ship yards have at least one drydock used for the maintenance and repair of ships and boats. Drydocks can be filled with water to allow a vessel to sail into it, and then drained leaving the entire body of the vessel exposed so that it can be worked on. Some drydocks are extremely large to accommodate massive ships in need of repair work. A skilled team of repair people work on the vessel while it is drydocked, who then flood the drydock so that the ship can return to open water. A marine drydock is subject to study and research from several points of view, such as environmental, hydrodynamic design and construction. The effect of drydocks on marine hydrodynamics is mainly related to the significant amount of pollutants that build up over drydock surfaces due to intensive industrial activity [1,2]. The construction of a drydock is a complex procedure, which needs to scientifically integrate management technology [3]. Special design concerns shall be considered for a drydock, such as marginal wharf structure [4,5] and also the control of drydock operations [6]. The special loading pattern on drydocks due to uplift pressure [7] and the interaction of marine hydrodynamics and structures [8-11], shall be considered. One of the main concerns in the design of drydocks is the total time required to fill it with sea water [12]. The filling time mainly depends on the specifications of the flooding system, which generally operates by gravity. The main components of a flooding system, such as the intake channel and guide walls are generally very complex. The hydraulic boundary conditions are also time variable because of the tidal variation of the sea water level. Interaction between drydocks and marine hydrodynamics and sedimentation is also a major issue in design [13]. So, it is necessary to investigate the hydrodynamic behavior of drydocks and also to inspect the flow

1. *Department of Civil Engineering, Tarbiat Modares University, Tehran, P.O. Box 14115-317, Iran.*
2. *Water Research Institute, Tehran, P.O. Box 16765-313, Iran.*
*. *Corresponding author. E-mail: a.jilani@modares.ac.ir.*

Received 15 December 2009; received in revised form 3 February 2010; accepted 7 June 2010

pattern and efficiency of their flooding systems. The application of numerical models is also an option to simulate water flow through the flooding system. The numerical models are preferred because they can be easily modified and optimized according to future changes. The numerical models shall be verified using experimental results under the same conditions. The complexity of boundaries in the flooding system of drydocks is one of the main issues of consideration in numerical modeling.

As per the authors review, experimental and numerical research on the flooding system of a drydock has not been carried out. So, the main objective of this work is to investigate the flooding system of an under design graving dock located on the southern coast of Iran, using both experimental and numerical models. An experimental model is developed and the flooding system of the graving dock under various conditions has been tested. A numerical model is also developed to simulate the flow pattern in the flooding system of the graving dock. The complex geometry and time-variable boundary conditions are completely simulated in the numerical model. The main goal of the experimental tests is to evaluate the required time for the flooding of the graving dock and the effects of the tidal variation of the sea water level on it. It was tested that the required time of flooding can be satisfied only by gravity or by need of an additional pumping system. Moreover, the water flow pattern in the intake channel of the flooding system is observed in the experimental tests. The bed, walls and ceiling geometry of the intake channel and its effect on water flow during the flooding of the graving dock are investigated based on laboratory observations. The current velocity and pressure are also measured in the tests and discussed. Some observational results, such as air trapping in the flooding channel are also investigated. The main goal of numerical modeling is to develop a changeable validated model that may be modified based on any future modifications. The numerical results are compared with the corresponding laboratory measured data and a good agreement is obtained. The numerical results are also investigated for water flow velocity and pressure.

SPECIFICATIONS OF FLOODING SYSTEM

The flooding system investigated here is located between two adjacent graving docks and is applied to fill both of them. The general location plan of two graving docks and their flooding system is shown in Figure 1. As shown in this figure, by the hatched area, the experimental model only includes the northern drydock as well as the flooding system; the southern drydock was not included in the laboratory and numerical model. The detailed specifications of the flooding system are shown in Figures 2 and 3. In Figure 2, a plan view of the system is illustrated. All the main parts of the system are characterized by a number. Longitudinal and cross sections of the flooding system are shown in Figure 3. The hatched area in this figure also indicates the boundaries of the experimental and numerical model. The numbering of the main parts of the flooding system is the same as in Figure 2. The definition of each numbered part of this figure is as follows: The entrance trash rocks at the mouth of the flooding system are indicated by numbers 1 and 2. The entrance gates used to control the seawater flow into the flooding system are indicated by number 3. The experimental and numerical tests were carried out for various opening percentages of these gates. The main seawater intake channel is numbered as 4. The barriers located at the bottom of the intake channel and the overflow bottom weirs are numbered as 5. These barriers cause the flow to fall down through the four bed openings of the intake channel. The lower stage of the flooding system with a sloped bed is numbered as 6, and its internal vertical guide walls are indicated as number 7. After passing the main intake channel and falling down via its bed openings, seawater flow guides towards the two adjacent drydocks due to the sloped bed of the lower stage. The seawater passes into four conveyance short pipes and lastly goes up from ten bed openings of the drydocks, indicated by number 8. The water surface in the graving dock is gradually raised

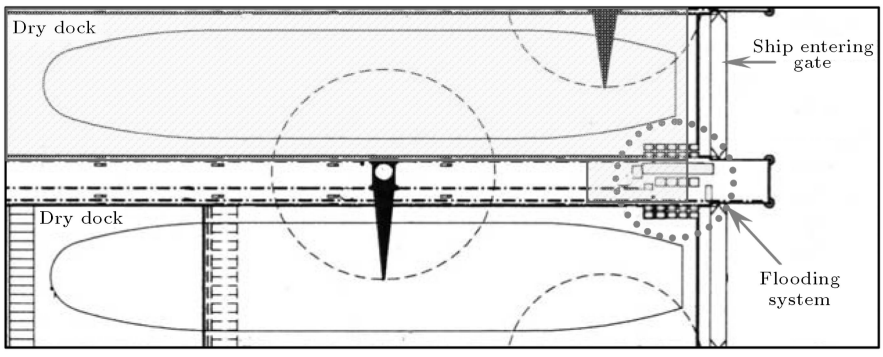

Figure 1. Central flooding system located between two adjacent graving docks. Zone of experimental modeling is hatched.

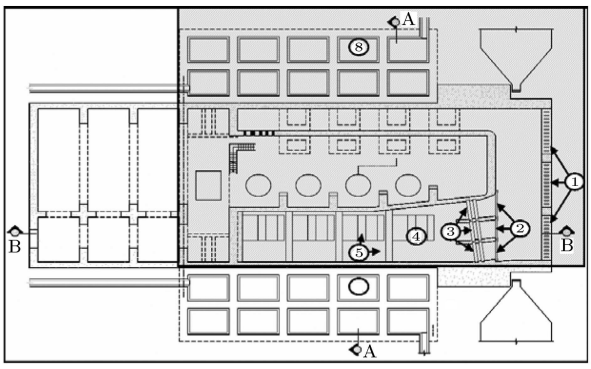

Figure 2. Plan view of flooding system. Numbers are described in the text and zone of experimental modeling is hatched.

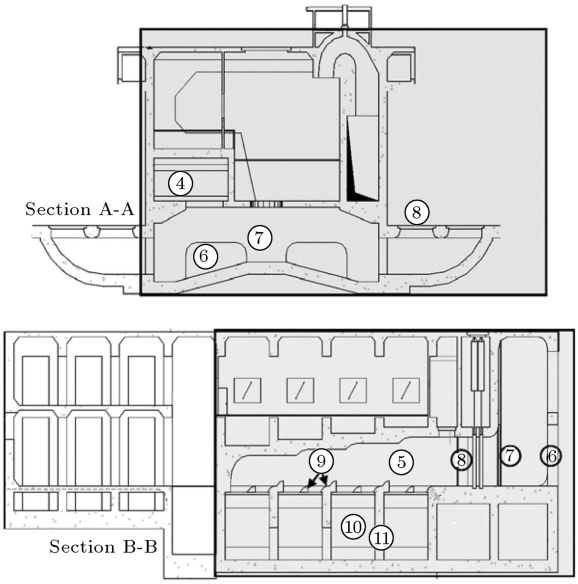

Figure 3. Cross sections of flooding system. Location of sections are indicated in Figure 2. Numbers are described in the text, and zone of experimental modeling is hatched.

due to water entering from its bed opening. When the water surface elevation is the same as the sea water level, the flooding procedure is finished. Detailed information about the experimental modeling of the flooding system, and the test specifications, are given in the following chapter.

As can be seen in Figures 2 and 3, the system is applied for both the flooding and dewatering of graving docks. Both systems are experimentally and numerically investigated, but only the investigation on the flooding system is presented here. Investigations regarding the dewatering system are under preparation in a separate manuscript.

EXPERIMENTAL MODELING

In this work, the experimental model of the flooding system was developed based on the similarity of the Froude Number in the model and prototype. So, turbulent water flow through the flooding system is controlled in the model. The appropriate scale ratio is selected to minimize scale effects in the model. Both the upstream and downstream boundary conditions of the flooding system are time variable. At the upstream, the water surface elevation varies according to tidal variation of the sea water level at the site of the project. This tidal variation is determined based on a tide table recorded at the nearest measuring station to the study area, and it is shown in Figure 4. At the downstream, the water surface in the graving dock is time variable due to gradual rising during the flooding stage. So, the hydrodynamic specifications of water flow in the intake channel are completely time variable. The maximum discharge from the sea into the drydock occurred at the start of flooding and it is decreased by raising the water level in the drydock. So, there is a time period at the end of the flooding stage during which the flow velocity is too low and so can be categorized as non-turbulent. This period of time shall be investigated in the experimental model. For this investigation, before developing the laboratory set up, the water velocity in the intake channel is determined based on the simple energy balance between up and downstream on the flooding system, considering the friction and local losses of the water head. Based on this simplified method, the variation of velocity and, then, the Reynolds Number (Re) of the water flow are determined during the flooding stage. This variation is shown in Figure 5. As seen in this figure, the Reynolds Number is decreasing by time, while the water surface rises in the drydock. The limit of turbulent flow, as Re = 2000, is shown in the figure and it can be seen that in prototype the laminar condition occurs in only about one percent of the flooding period. This result is

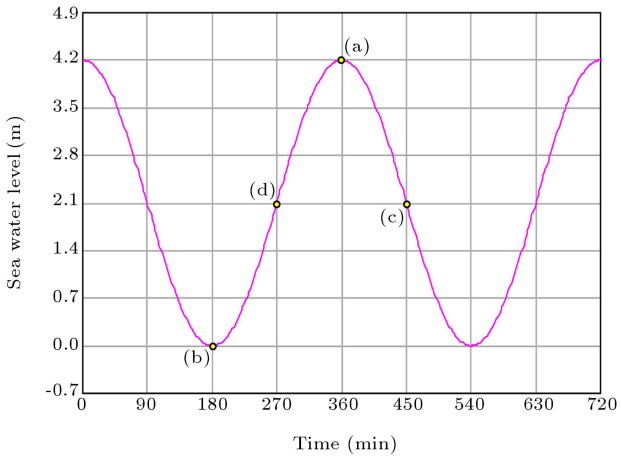

Figure 4. Tidal variation of sea water level as the upstream boundary condition of the flooding system points. (a) to (d) show the sea water level at the start of flooding in different experimental tests.

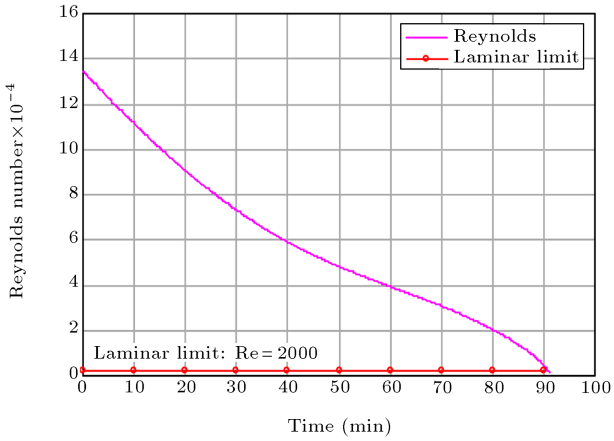

Figure 5. Variation of minimum Reynolds Number in the intake channel of the flooding system.

used to select an appropriate scale for the experimental model. Based on the investigations, it is concluded that by selecting a scale as 1:16 or smaller, the laminar period is about one percent of the total flooding stage, as occurred in the prototype. But for greater scales, such as 1:15, the laminar period will be increased up to 10 percent of the flooding stage, which can increase scale effects on experimental measurements. So, the scale of the experimental model is selected as 1:16.

After checking flow turbulence in the experimental model, as mentioned above, the model was designed and constructed based on the similarity of the Froude Number in model and prototype. Based on the Froude law of similarity, the modeling scale or the ratio of model to prototype for each of the parameters was determined. Using the scale factor as $L_r = 1:16$, the time ($L_r^{0.5}$), the discharge ($L_r^{2.5}$), velocity components ($L_r^{0.5}$) and the pressure (L_r) were scaled based on the Froude law of similarity. The Froude scaling law was applied to upscale all experimental measurements, such as water pressure and velocity, as well as flow discharge into the intake channel from the model to the prototype. The up-scaled values were applied to evaluate the flow pattern and filling rate of the dry dock as will be explained later.

Based on the selected scale, the experimental model of the graving dock was constructed for the area hatched in Figures 1 to 3. The model of the flooding system was built using different materials, such as wood and Plexi-glass. The bed and the guide slopes were wooden, and the walls and ceiling of the flooding system were built using clear Plexi-glass. The model of the graving dock was built using masonry material. A one tail gate was installed at the downstream of the drydock to flush out the water. A sharp crested weir was also installed at the downstream of the tail gate to measure water discharge in the flooding system in steady state experimental tests, which are described later. An upstream reservoir was also modeled to simulate the sea water level as the upstream boundary condition of the flooding system. The water pumped into this reservoir and its level are controlled to be exactly according to the tide variation of the sea water level in the prototype. Figure 6 shows an overview of the experimental model including the graving dock and its tailgate, upstream reservoir and flooding system. The experimental model of the flooding system is shown in detail in Figure 7. The flooding procedure in this figure is also illustrated, which will be discussed in the following section. The performed experiments can be classified into two categories: steady and unsteady tests. In steady tests, a fixed difference was created between up and downstream water levels of the flooding system. The water surface in the graving dock was fixed using its tailgate. The water level at the upstream reservoir was also fixed. In this condition and for various differences between up and downstream water levels, the water discharge into the drydock through the flooding system was measured. Moreover, the pressures on the bed, walls and ceiling of the intake channel were measured for the maximum water level

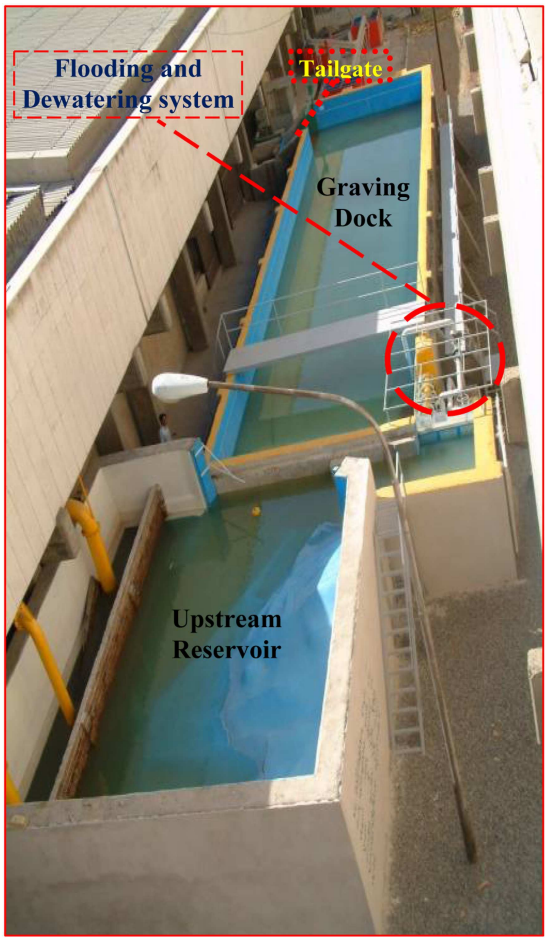

Figure 6. Overview of main components of experimental model: graving dock, upstream reservoir and flooding system. View of flooding system is shown in Figure 7.

difference. The exact locations of the piezometers are shown in Figure 8. In unsteady tests, the water level in the upstream reservoir was exactly varied on the scaled tidal variation of sea water. The flooding in the unsteady tests is completed when the water level in the graving dock is equal to the water level in the upstream reservoir. The flow pattern in the flooding system was observed and investigated in unsteady tests. The variation of water surface elevation in the graving dock was also measured to investigate the required time for complete flooding. Four different states of sea water level at the start of flooding were considered

Figure 7. Experimental model of flooding system and various flooding stages of graving dock. (a) Free surface flow at the beginning, and (b) intermediate condition from free surface into pressurized.

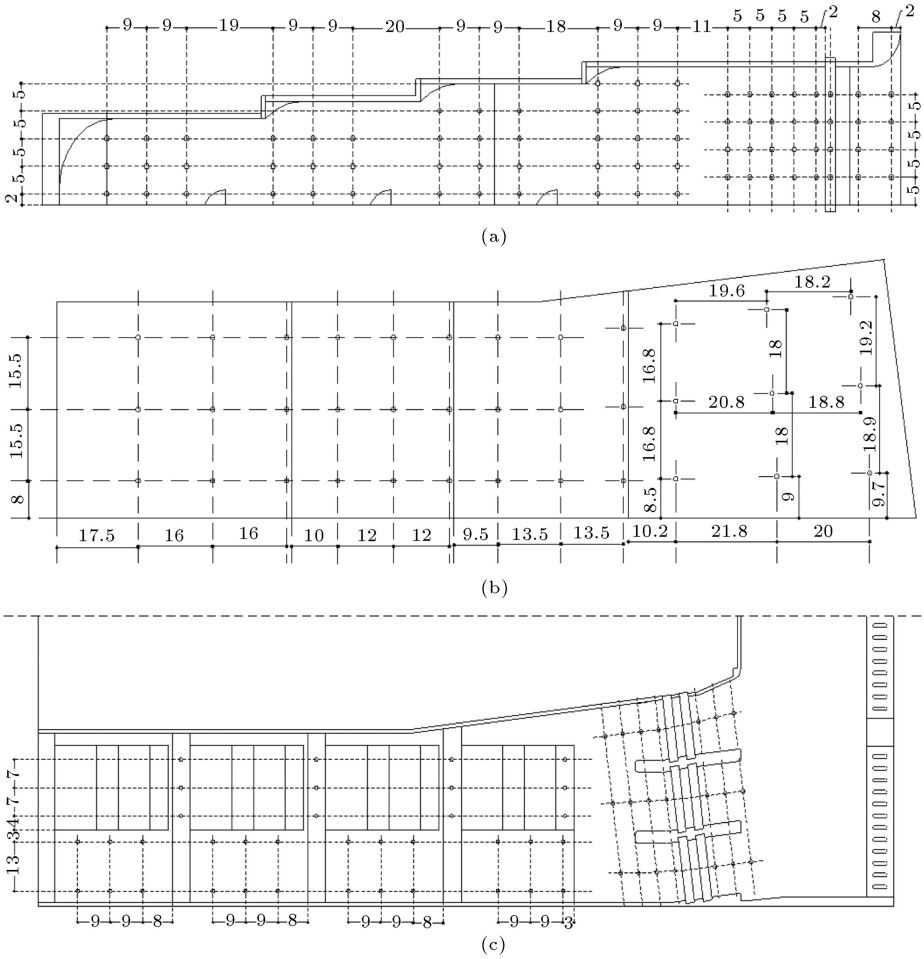

Figure 8. Piezometers locations in the intake channel of flooding system. (a) Wall; (b) bed; and (c) ceiling of channel.

in unsteady tests. These four states are as follows: highest high water level, lowest low water level, average water level during the ebb condition and average water level during the flood condition. These statuses are indicated by points (a) to (d) in Figure 4, respectively. Each experimental test was repeated at least twice to minimize probable errors. The results measured in steady and unsteady tests were compared to achieve the maximum reliability of measured data.

NUMERICAL MODELING

More investigation into the flooding system of the drydock is made developing a numerical model. Numerical modeling is made using the finite element method to simulate the complex geometry of solid boundaries in the intake channel. The main goal of numerical modeling is to investigate the water pressure and current velocity domain in all the flooding system to double check the measured data about water discharge into the system and water pressure on the bed, walls and ceiling of the intake channel. The numerical model can be also used for any probable modifications that are required to optimize flooding efficiency or to streamline boundaries in the intake channel. Dimensions in the numerical model are scaled and, so, are completely similar to the experimental model. The results for using the prototype are scaled up according to each parameter. The main components of the numerical model of the flooding system are shown in Figure 9.

Mesh generation of the numerical model is made using a tetrahedral element. This element is nonlinear and three dimensional, which is recommended for simulation of steady state and transient water flow. The degrees of freedom for this element are defined as water current velocity, pressure and temperature. Water flow through the flooding system is only simulated in its pressurized form, and the initial free surface and intermediate phases are neglected in the numerical modeling. Element dimensions and arrangements are optimized after several attempts to produce the best and fastest convergence in the modeling stage. In total, 23372 nodes and 108421 elements are applied in the final mesh generation.

The numerical solver is evaluated to select appropriate techniques of simulation of sea water flow through the intake channel of the drydock. Based on the literature recommendation, four types of element shape can be selected in the numerical solver: hexahedral, tetrahedral, wedge and pyramid. Figure 10 shows the possible shapes of elements in the numerical model. Based on analysis of results using various options of the element shape, it was concluded that wedge and pyramid options with 5 faces are not suitable for simulating complex geometries of the rigid boundaries of the flooding system. The hexahedral option is applicable but leads to more computational time and increases the sensitivity of the solution and the probability of divergence in the element dimensions. The tetrahedral option was recognized as the most suitable element shape, which was carefully able to define the complex geometry of the boundaries and the rational behavior in simulation convergence.

For this element, the program calculates velocity components and pressure from the conservation of three properties: mass, momentum and energy. The conservation equations for viscous fluid flow and energy are solved in the fluid region, while only the energy equation is solved in the non-fluid region. The material number of elements was equal to one for fluid elements and greater than one for non-fluid elements. The dimensions of the elements were varied from 1.5 cm for locations with complex geometry to 4 cm for simpler

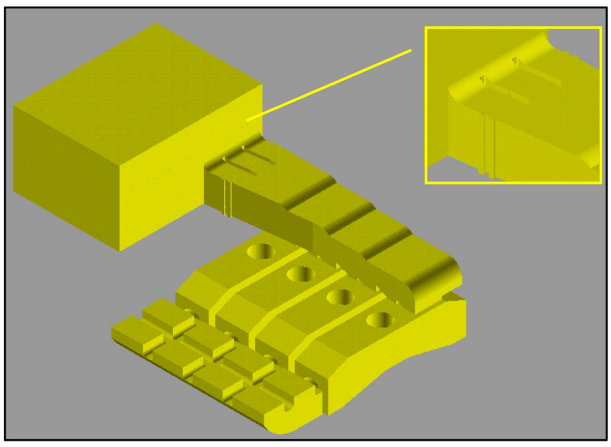

Figure 9. Numerical model of drydock flooding system; boundary geometry is according to Figures 2 and 3.

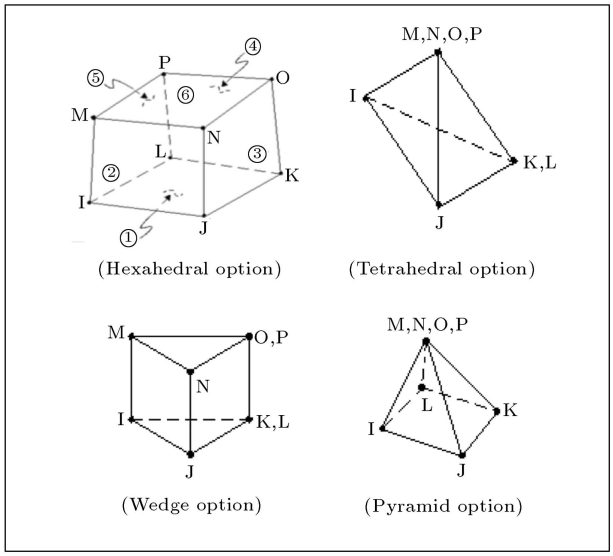

Figure 10. The shape options for elements in numerical model.

geometries, such as upstream fluid reservoirs, which simulate the seawater upstream boundary condition. The analysis shows that the greater dimensions of the elements can lead to divergence of the numerical simulation. Also, in smaller elements, the accuracy of numerical results will not strongly increase. The accuracy of the numerical results (compared with corresponding experimental data) will increase only about 5% by decreasing about 50% of the element dimensions from the selected values. Moreover, it was concluded that the rate of changing element dimension should not be steep. The maximum applicable rate of changing the dimension of the element, especially at the entrance of the intake channel, should not be more than 18% between two adjacent elements. In the applied simulation technique in this work, the velocities are obtained from the conservation of momentum principle, and the pressure is obtained from the conservation of mass principle. A segregated sequential solver algorithm is used, that is the matrix system derived from the finite element discretization of the governing equation for each degree of freedom of the fluid element in the intake channel is solved separately. The flow pattern is nonlinear and the governing equations are coupled together. The sequential solution of all the governing equations, combined with the update of unsteady boundary conditions in up and downstream, constitutes a global iteration.

A numerical solution of the Navier-Stokes equations for turbulent flow was carried out. Due to the significantly different mixing-length scales involved in turbulent flow through the intake channel of the drydock, the stable solution of this requires such a fine mesh resolution that the computational time becomes significantly infeasible for calculation. So, as an alternative, and for including the effect of turbulence in numerical modeling, the calculations were also done using Reynolds-Averaged Navier-Stokes (RANS) equations supplemented with a $k-\varepsilon$ turbulence model. The numerical accuracy of the results, as well as the required time of simulation at each time step, was compared. Based on the analysis of the results of this work and a review of similar numerical modeling of pressurized flows [14,15], it was concluded that the well-known RANS equations with a $k-\varepsilon$ turbulence model in an unsteady condition for water as an incompressible Newtonian fluid can be applied as the main governing equations in the numerical model, and can be a recommended option for any similar flow simulation problem. The technique of a numerical solver in analysis of nonlinear partial differential equations and boundary conditions is trial and error. A preliminary answer is assumed at each effort and gradually corrected to achieve the best answer, which satisfies domain equations and boundary conditions with minimum error. So, the trace of the iteration procedure in the numerical solver is one of the main concerns. In this work, the trace of iteration was made, using Graphical Solution Tracking to evaluate the rate of convergence of the simulation. The convergence rate (P) of each of the main variables is calculated using the following equation:

$$P = \frac{1}{m}\left(\sum_{1}^{m}\frac{\phi_n - \phi_{n-1}}{\phi_n}\right), \tag{1}$$

where ϕ_n is the value of the variable (such as water pressure or velocity components) in the nth iteration, and m is the number of nodes. Based on this technique, the variation of convergence rate with the number of iterations for three components of water velocity in the flooding system is shown in Figure 11. As seen in this figure, 100 iterations were determined as a safe number of iterations for minimizing numerical errors in the trial and error technique and, in more iterations, the efficiency of the solution will be decreased due to an increase in computation time. It shall be considered that the convergence of the simulation was mainly based on an optimization of mesh dimension and time step, and that, subsequently, the best iteration number of the solution shall be determined using the above mentioned technique.

The boundary condition in the flooding system was defined as the geometry of solid boundaries of the intake channel. The normal velocity vector perpendicular to the solid boundaries was fixed as zero. All geometrical boundaries were simulated according to prototype specifications. Moreover, the upstream boundary condition of the flooding system was according to the tidal fluctuations of the sea water level. At the downstream, water surface elevation in the drydock is applied. This elevation is computed at each time step, based on water discharge through the flooding system at the previous time step. The time steps

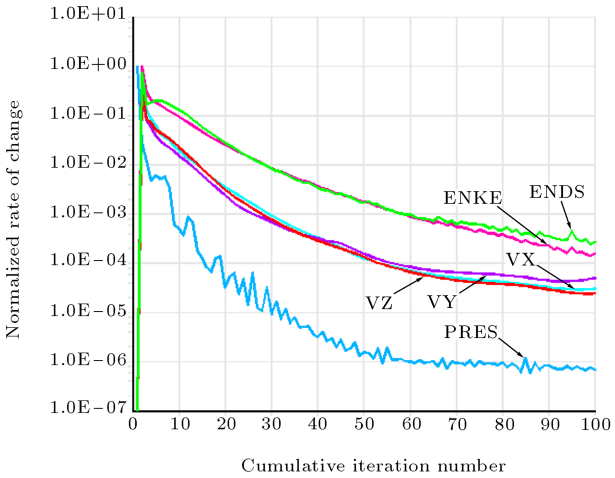

Figure 11. The variation of convergence rate with various iteration numbers in numerical simulation.

are selected small enough to eliminate effects of time lag of the calculated water level in the drydock on numerical results. The exact time step was determined as 0.1 s, to eliminate the effect of time steps on numerical results. In the simulation procedure, the accuracy of the solution is cared. As iteration is used to determine the main degree of freedom (water velocity and pressure) in each element, the convergence of simulation and the high accuracy of results are optimized. Figure 12 shows the generated mesh in the numerical model in all flooding systems.

Water pressure and the current velocity domain are the main results of the numerical model. The results are obtained under the same corresponding conditions as explained for unsteady tests in experimental modeling. Sample results of water current velocity vectors are illustrated in Figure 13 for totally opened entrance gates while the sea water level at the start of flooding is according to the highest high water level as indicated by point (a) in Figure 4. The maximum water velocity in the flooding system is occurred in this case. The figure shows the velocity vectors ten minutes after the start of flooding.

RESULTS AND DISCUSSION

The main concern of this work is experimental investigation into the flooding system of drydocks. A numerical model is developed to generate a changeable model for any future modifications. So, inspection of results begins with investigations into the measured data and experimental observations. Firstly, water discharge from the sea into the graving dock is inspected, based on the recorded water level in the drydock during unsteady tests. This investigation is undertaken for various sea water levels at the start of flooding and

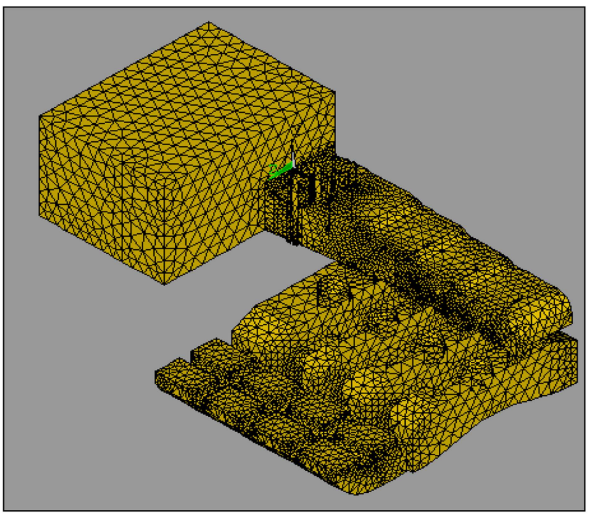

Figure 12. Mesh generation in the numerical model of drydock flooding system.

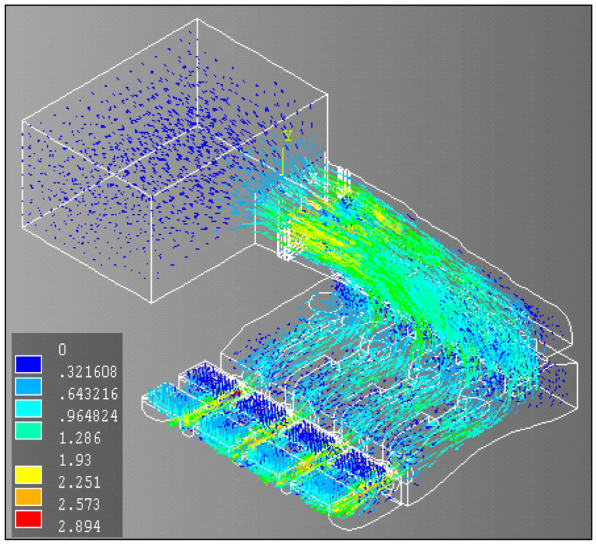

Figure 13. Numerical results for scaled up water current velocities (m/s) in the drydock flooding system.

various opening percentages of the entrance gate. The results are shown in Figure 14. As can be seen, the rising rate of the water level decreases during the flooding stage. In case (a) where the flooding starts at the highest high water level (point (a) in Figure 4), the minimum time period required to fill the drydock is about 60 min, and the maximum water depth in the dry dock is about 12 m, as illustrated in Figure 12a. The effect of the opening percentage of the entrance gate on the required time of filling is also illustrated in Figure 14. For instance, when the flooding is started at the highest high water level, reducing the opening of the entrance gates from 100% to 50% causes about a 30% increase in the required time for filling. The worse case is occurred when the flooding starts at the lowest low water level, according to point (b) in Figure 4. In this case, the minimum required time of filling the drydock is about 120 min. It is important that the opening percentage of the entrance gate is not very effective on the reduction of flooding time. The effect of the opening percentage of the entrance gate on flooding time is less than 5% in case (b). It can be concluded that if the start of flooding is according to the lowest low water level in tidal variations of the sea water level, a booster pumping is needed to accelerate the filling rate of the drydock and reduce flooding time. In case (c) where the flooding started at the average sea water level during the ebb, the water depth in the drydock will have a maximum value of 9.7 m. The effect of the gate opening on flooding time is also negligible in this case. The required time for filling the drydock up to the maximum available water level is about 70 min, and it seems that booster pumps are needed to increase the rate of filling in this case [16,17]. In case (d) where the flooding started at the average sea water level during the tide, the condition is generally similar to case (a).

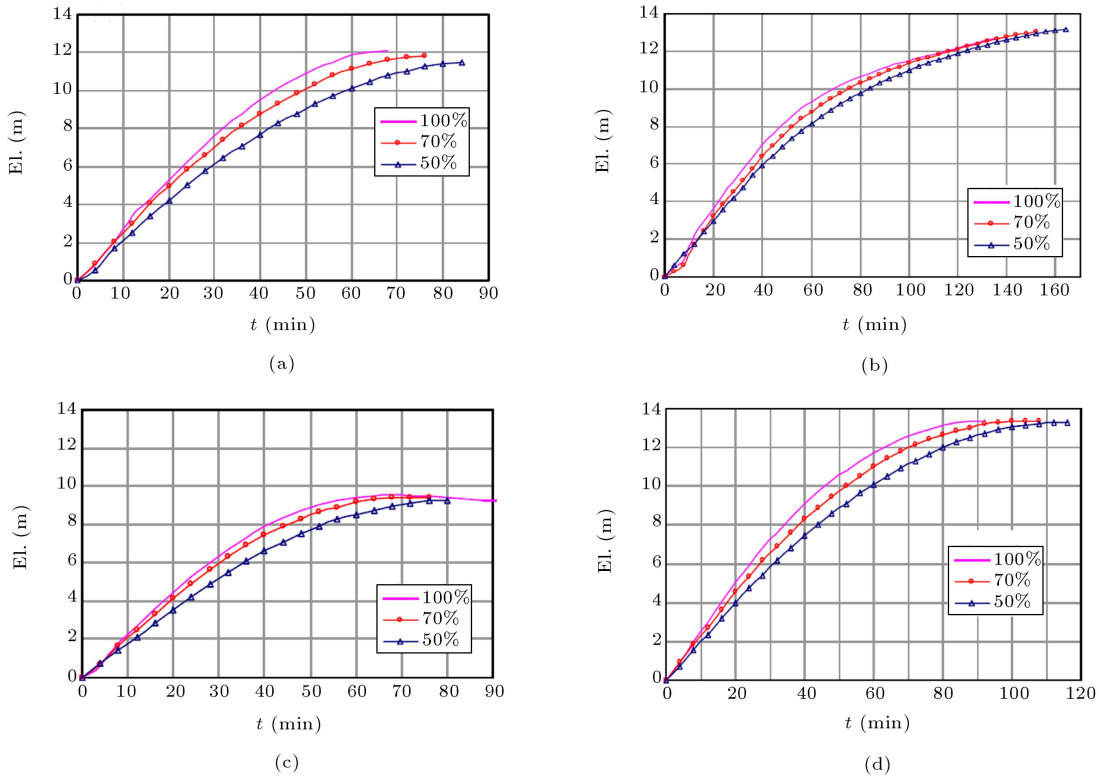

Figure 14. Scaled-up values of water surface elevation in graving dock for various opening percentage of gate as 100, 70 and 50%. Cases (a) to (d) show the sea water level at the start of flooding as indicated in Figure 4.

The minimum flooding time for full opened entrance gates is about 60min. The closing half of gates leads to about 30% increase in the filling time. The maximum water depth in the drydock exceeds other cases, but the water depth at 12m is assumed as the filling of the dry dock.

For more investigations, the time variation of water discharge into the flooding system is determined for several cases, (a) to (d), in unsteady tests. The results are illustrated in Figure 15. As seen in the figure, the water discharge decreases while the water surface increases in the drydock. The minimum water discharge occurs for case (b) when the sea water elevation at the start of flooding is the lowest low. The effect of the opening percentage of the entrance gate on the water discharge is generally the same as indicated in Figure 14. The maximum difference for water discharge into the drydock is about 15% and observed between cases (a) and (b). At about the first half of the flooding time period, the water discharge for lower openings in the entrance gates are clearly less. But after a recognizable point (named point "o" in Figure 15) the water discharge for lower gate openings is more. The reason is that, in lower opening cases the raising of the water level in the drydock has a lower rate. So, in the second half of the flooding period, the difference between the water level in up and downstream (sea water level and water surface in dry dock) in lower opening cases is more, and leads to more discharge. This point is generally in accordance with half the time of the flooding period in cases (a) and (d). There is not a similar clear point in cases (b) and (c), but the general variation of water discharge is the same.

To verify the measured values in unsteady tests, such as water discharge into the drydock, the measured values in unsteady tests are compared with the steady test records. This comparison is shown in Figure 16. Water discharge into the flooding system was measured in steady tests for various water head differences between up and downstream (sea and graving dock). For comparison, the water head difference between up and downstream in each case, (a) to (d), is determined. Then, by fixing the water level in the upstream reservoir and in the dry dock, the water discharge into the drydock is measured. So, the measured data in each case is compared as illustrated in Figure 16. A good agreement is observed between measured data in steady and unsteady tests and confirms the results concluded from measured data in unsteady tests.

In steady tests, when a fixed water head difference is dominated in the experiments, the water pressure on the bed, walls and ceiling of the intake channel is measured at the piezometer locations. The water pressures are measured only for maximum water head differences between up and downstream of the flooding system. The measured pressures are illustrated in

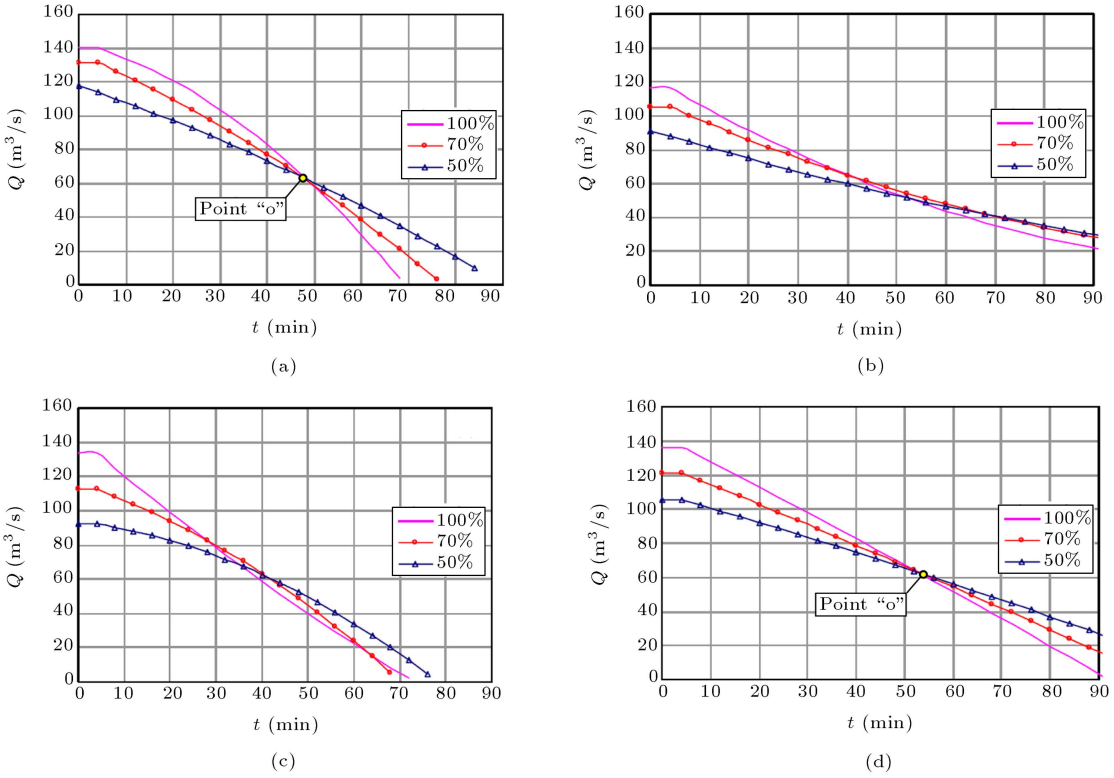

Figure 15. Scaled-up values of water discharge into the graving dock during operation of flooding system for various opening percentage of gate as 100, 70 and 50%. Cases (a) to (d) show the sea water level at the start of flooding as indicated in Figure 9.

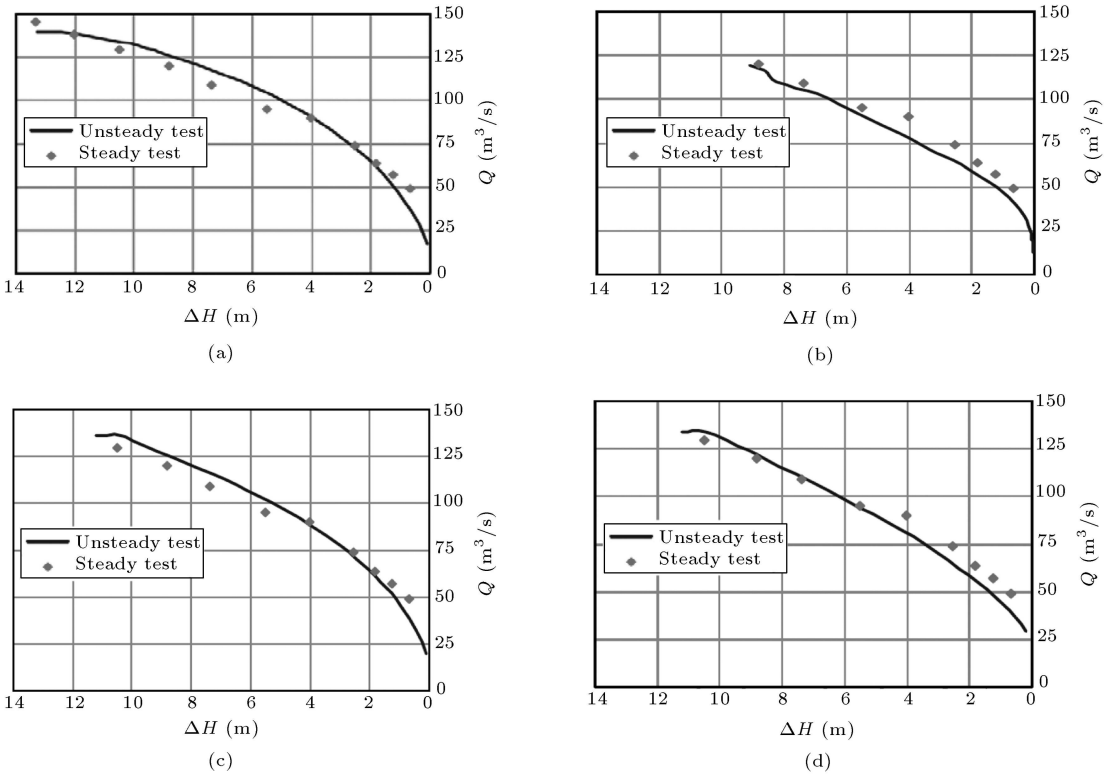

Figure 16. Comparison of water discharge into the flooding system measured in steady and unsteady tests for various water head difference between up and downstream (sea and graving dock). Cases (a) to (d) show the sea water level at the start of flooding as indicated in Figure 9.

Figure 17. According to Figure 17a, at the walls of the intake channel, a regular stratified pressure domain is observed, which does not have a major variation in all the length of the channel. Local upraising in water pressure is measured around the guide overflow weirs located at the bed of the channel. The maximum water pressure on the walls is about 26 water centimeters. The water pressure on the walls at the beginning of the channel immediately after the entrance gates is relatively less. In Figure 17b, the water pressure at the bed of the intake channel is illustrated. As can be compared, water pressure on the bed has generally a different pattern relative to the walls. A major variation of bed water pressure can be seen in all the length of the intake channel. At the points which have more distance from the entrance gates, water pressure is gradually increased. The water pressure on the bed at the end of the channel is about 33 water centimeters, which shows about a 30% increase relative to maximum wall pressure at 26 water centimeters. It may be due to high water velocity at the initial parts of the intake channel and low order velocity at its downstream parts. It seems that the main water discharge passes through the first and second bed openings of the intake channel and the other two downstream openings play a minor role at the flooding stage. This unbalanced pattern should be modified using small or streamlined guide overflow weirs on the bed to moderate the resistivity against the flow kinetic energy in the intake channel. At the ceiling, as illustrated in Figure 17c, a generally uniform water pressure is measured. But, some local increasing in water pressure is observed due to the effect of guide overflow, causing the water current to reflect toward the roof of the channel. The major increasing effects are shown at the beginning of the intake channel, which is about 10%. This local rising in water pressure should be considered in the construction material of an intake channel, as well as the surface lining.

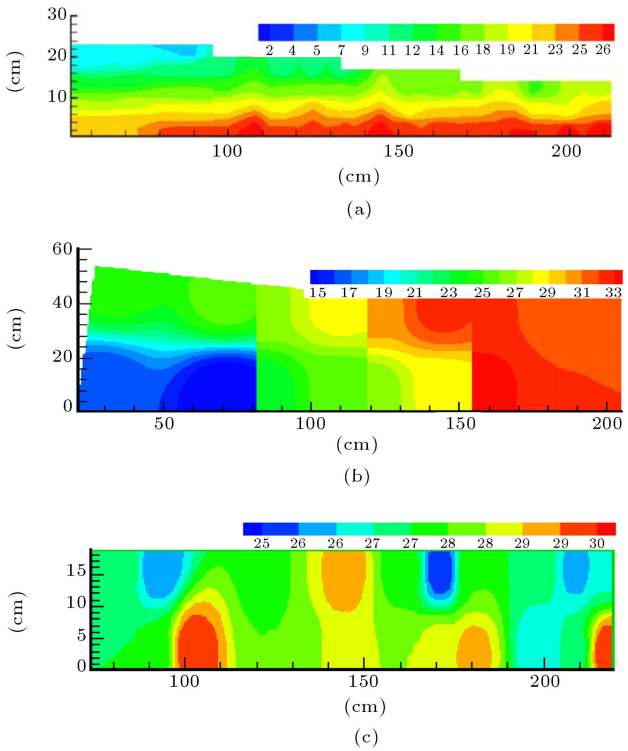

Figure 17. Water pressures measured at (a) wall, (b) bed and (c) ceiling of the intake channel of flooding system. All pressure is in water centimeters.

Lastly, some laboratory observations are made about the flow pattern in the flooding system of graving docks. As illustrated in Figure 18, air trapped at the top of the intake channel is a major issue, which is observed in all cases in unsteady tests. It occurs due to the non-streamlined geometry of boundaries at the ceiling of the flooding system. Modification of the roof geometry can minimize the air being trapped in the prototype, increase the discharge capacity of the intake channel and decrease the filling time of graving docks in all cases. Moreover, it is observed that the water flow at the start of flooding is free surface. The time period of free surface flow is about 5 to 7% of the total flooding time in all test cases. Passing an intermediate state, the flow changes, being pressurized in the intake channel, as illustrated in Figures 7a and 7b. It is observed that the probability of destruction and cavitation is high under free surface and intermediate flow conditions.

After a detailed investigation into experimental measurements, the inspection of results is focused on the numerical model. As mentioned, the main goal of numerical modeling is to develop a verified and reliable model of a flooding system that can be applied for any future changes in geometry or boundary conditions. So, to verify the numerical model, a comparison is made between experimental and numerical data under

Figure 18. Trapping of air at the top of intake channel due to non-streamlined geometry of boundaries at ceiling of flooding channel.

the same conditions. The comparison is made for water pressure on the solid boundaries of an intake channel and also for water discharge passing through the flooding system. Figure 19 shows the comparison of numerical results and measured data in a physical model for water pressure on the ceiling, walls and bed of the intake channel.

A good agreement is obtained between numerical and experimental models. As seen in Figure 19a, the measured water pressure on the ceiling of the intake channel is generally more than numerical results. It seems that the effect of bed barriers, such as guide overflow weirs, on the flows cannot be completely simulated in the numerical model. The deviation from measured values is about 10%. An inverse status can be seen in Figure 16b, for water pressure on the bed of the intake channel. The calculated values are about 10% greater than measured data in the experimental model and it seems that water velocity near to the bed of the channel is more than numerical results, and also flow separation from the bed, which may be caused by bed barriers, cannot be completely simulated in the numerical model. The measured water pressure on the walls is generally the same as numerical results, as shown in Figure 16c. A comparison of numerical and experimental results is also made for water discharge into the flooding system for case (a) when the sea water level is the highest high water at the start of flooding. Two opening percentages of entrance gates are considered as 100 and 50%. As seen in Figure 20, water discharge in the laboratory model is generally the same as calculated data. It should be noted that both axes of graphs in Figure 20 show non-scaled up values. The scaled up experimental values of water discharge vs. time in this case were illustrated in Figure 15a.

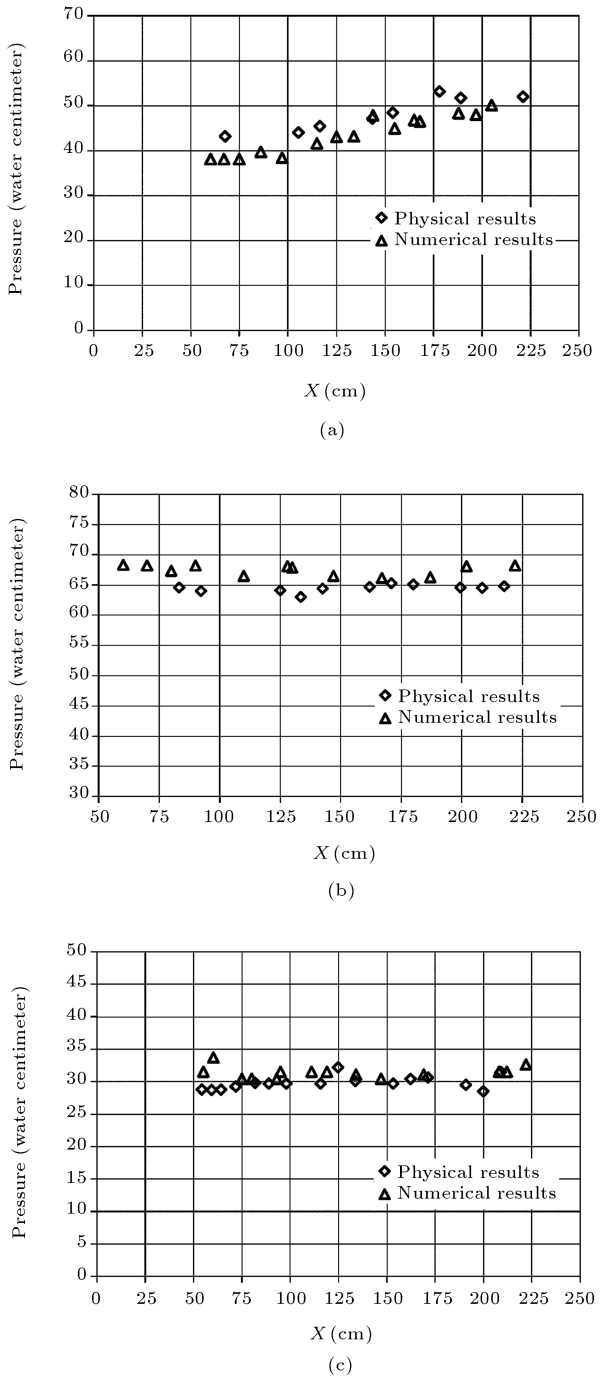

Figure 19. Comparison of numerical and experimental (physical) results for water pressure on ceiling (a), bed (b), and wall (c) of intake channel.

As shown in Figure 20, a maximum deviation from experimental measurements is observed at the start of flooding in the numerical model. The calculated water discharge in the numerical model is generally higher than the measured data in the physical model. It occurs due to different flow conditions in the experimental and numerical model. As explained in laboratory observations, seawater flow in the intake channel is initially free surface, which cannot be modeled in the numerical investigation. It can be concluded that the free flow stage at the start of flooding leads to a reduction in discharge capacity and causes an increasing in flooding time.

The first result to be concluded from numerical modeling is that the procedure explained here can be recognized as a successful method for numerical simulation of sea water current in the intake channel. Moreover, maximum water velocity is determined to check related limitations. As shown in Figure 21, the maximum water current velocity is calculated as 2.85 m/s in the model, which is equivalent to 11.6 m/s in the prototype. This maximum water velocity is less than the maximum allowable velocity in the pressurized channels as 16 m/s [16].

An investigation into numerical results is also undertaken on the water pressure domain in the intake channel. As shown in Figure 22, the general pattern of water pressure in the channel is hydrostatic, but some fluctuations are observed around the internal guide

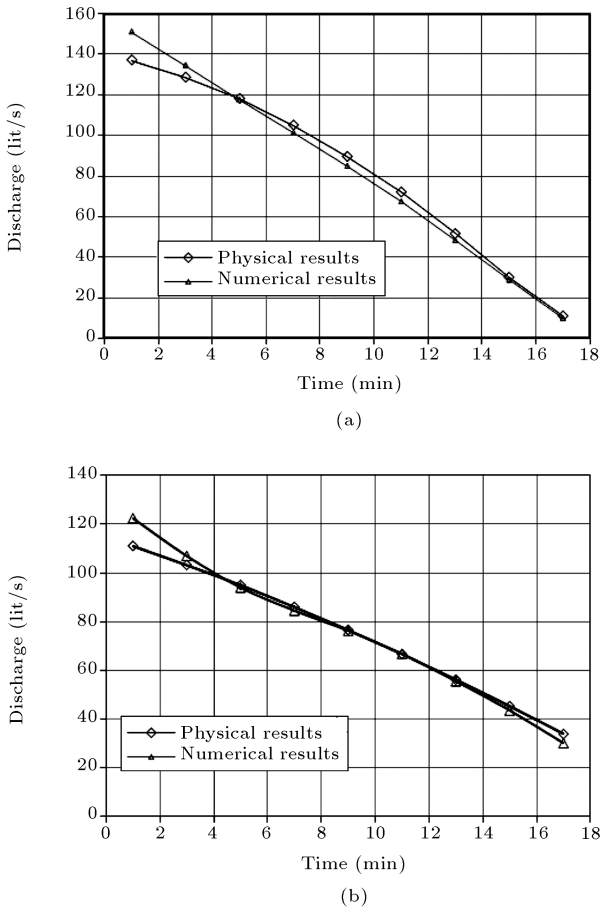

Figure 20. Comparison between experimental and numerical results for water discharge variation vs. time during flooding stage. (a) 100% and (b) 50% opening of gates.

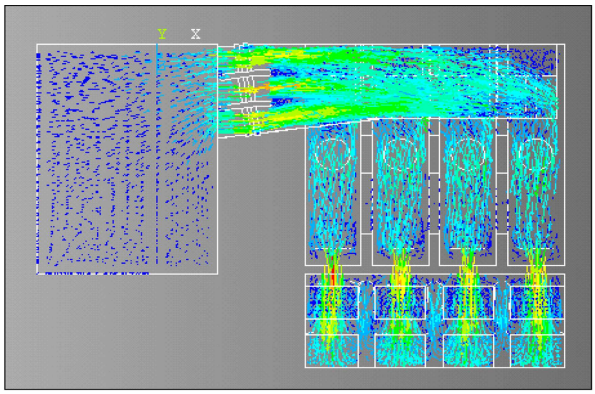

Figure 21. Plan view of flooding system and water velocity domain calculated by numerical model.

overflow weirs. The comparison between numerical and experimental results shows that the local effects of these internal barriers are not exactly simulated in the model. But, the deviation is generally less than 10% at maximum value and good agreement is obtained for the entire pressure domain.

Generally, it can be concluded that the present approach to the numerical modeling of water in the flooding system in drydocks can generate reliable results. Seawater characteristics in the flooding system are generally investigated. The verified numerical model can be used for any future changes to be made in the geometry of the flooding system or boundary conditions.

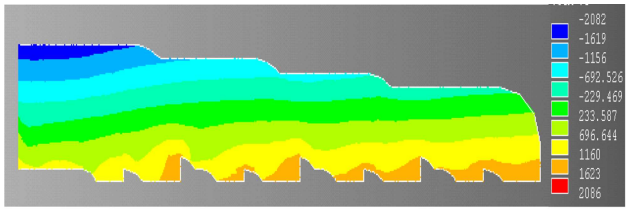

Figure 22. Cross view of intake channel and water pressure domain calculated by numerical model.

CONCLUSIONS

Laboratory investigations and numerical modeling have been carried out on the flooding system of an under design drydock located on the southern coasts of Iran. The main goals of the investigation are to evaluate flooding time, as well as flow specifications and patterns in the intake channels. The laboratory model is made based on the equivalent Froude Number in the model and prototype. The time variable upstream and downstream boundary conditions of the flooding system are completely modeled. The results include the required filling time of the drydock and also the water pressure domain on the bed, walls and ceiling of the intake channel. Various conditions for sea water surface elevation are considered to recognize the worthy case of the flooding stage and the maximum required time of flooding. It is concluded that if flooding started when the sea water level is equal to the lowest low water level, a booster pumping is needed to accelerate the filling rate of the drydock and reduce flooding time. The opening percentage of the entrance gate is not very effective in reducing flooding time. The effect of the opening percentage of the entrance gate on flooding time is less than 5% in this case. The investigation into water pressure on the intake channel shows that, at the walls of the intake channel, a regular stratified pressure domain is occurs, which does not vary greatly in all the length of the channel. Local upraising in water pressure is measured around the guide overflow weirs located at the bed of the channel. The water pressure on the bed has a generally different pattern relative to the walls. A major variation of bed water pressure can be seen in all the length of the intake channel. At the points which have more distance from the entrance gates, water pressure is gradually increased. Laboratory observations are also investigated. It is observed that trapped air at the top of the intake channel is a major issue observed in

all cases in unsteady tests. It occurs due to the non-streamlined geometry of boundaries at the ceiling of the flooding system. It is observed that water flow at the start of flooding is free surface. The time period of free surface flow is about 5 to 7% of total flooding time in all test cases. Passing an intermediate state, the flow becomes pressurized in the intake channel, as illustrated in Figures 7a and 7b.

The numerical model is developed using the finite element method to generate a changeable model for any future modifications. Numerical results are compared with laboratory measurements for water discharge into the drydock and for the water pressure domain on the intake channel boundaries. A good agreement is obtained between numerical and experimental results and a verified and validated model is obtained. The maximum differences between numerical and laboratory data especially for water discharge into the drydock, occurs at the start of flooding because of the different flow pattern at this stage in the numerical and experimental model. It seems that the reduction of discharge capacity is caused by the initial free surface flow. It is generally concluded that the probability of destruction and cavitations is high under the free surface and intermediate flow condition in the flooding system.

ACKNOWLEDGMENT

The support of the Water Research Institute (WRI), Ministry of Power of the Islamic Republic of Iran, is appreciated. Mr. A. Nik-Khah, Mr. M. Babaie, and Mr. M. Hatami, the WRI coastal engineering specialists, are especially greatly appreciated for their assistance in experimental investigations. Support of the Iranian Ship Buildings and Offshore Industrial Complex (ISOICO) is also appreciated.

REFERENCES

1. Akan, A.O., Schafran, C.G., Pommerenk, P. and Harrell, L.J. "Modeling stormwater runoff quantity and quality from marine drydocks", *J. of Envir. Eng.*, **126**(1), pp. 5-11 (2000).
2. Kretzschmar, R. "Best management practices for Oregon shipyards", *Tech. Report, Submitted to Oregon Department of Environmental Quality*, USA, pp. 90-110 (2000).
3. Kumamoto, T., Kameda, H., Hoshiya, M. and Ishii, K. "Construction of difficult dry dock in Yokohama, Japan", *J. of Constr. Eng. and Man.*, **116**(2), pp. 201-220 (1990).
4. Thibeaux, J.F., Nicolae Fratila, P.E., David M., Knuckey, P.E., Michael, B. and Endley, S.N. "Design issues for marginal wharf structures", *Conference on Port Development in the Changing World*, **2**, USA, Houston, pp. 1-9 (2004).
5. Arroyo, B., Hanganu, A.D. and Miquel, C.J. "Optimum design of multicellular reinforced concrete box docks", *J. of Struc. Eng.*, **128**(5), pp. 603-611 (2002).
6. Regan, J.E., Davies, S., Valdez, M.E. and Bradford W. "Automated monitoring system used to support drydock operations at electric boat", *Conference on Field Measurements and Geomechanics (FMGM)*, **1**, Boston, USA, pp. 1-11 (2007).
7. Kinner, E. and Stimpson, W. "Artesian pressure relief for trident drydock", *J. of Constr. Eng. and Man.*, **109**(1), pp. 74-88 (1983).
8. Fernandes, J. and Correia, R. "Structural behaviour of a dry dock with pile-anchored bottom slab", *J. of Mater. and Stuc.*, **19**(5), pp. 379-389 (1986).
9. Lai, C.P. and Lee, J. "Interaction of finite amplitude waves with platforms or docks", *J. of Watrwy., Port, Coast. and Oc. Eng.*, **115**(1), pp. 19-39 (1989).
10. Shugar, T., Holland, T.J. and Malvar, L.J. "Advanced finite element analysis of drydocks and waterfront facilities. A technology assessment", *Tech. Report No. A496342, Submitted to Naval Civil Eng. of Hueneme Port*, Canada, pp. 130-160 (1991).
11. Cheng, Y.S., Au, F.T., Tham, L.G. and Zeng, G.W. "Optimal and robust design of docking blocks with uncertainty", *J. of Eng. Struc.*, **26**(4), pp. 499-510 (2004).
12. JLARC "Review of port angles graving bock project", *Tech. Report No. 06-8 Submitted to the Joint Legislative Audit and Review Committee*, USA, pp. 200-294 (2006).
13. Seelam, J.K. "Drydock orientation and its effect on hydrodynamics and sediment transport in a macrotidal environment", *7th Conference on Coastal and Port Eng. in Developing Countries COPEDEC VII*, **1**, Dubai, UAE, pp. 28-43 (2008).
14. Eggels, J.G.M., Westerweel, J., Nieuwstadt, J. and Adrian, R.J. "Direct numerical simulation of turbulent pipe flow", *J. of Ap. Sci. Res.*, **51**(1), pp. 319-324 (2005).
15. Panton, R.L. "Review of wall turbulence as described by composite expansions", *J. of Ap. Mech. Rev.*, **58**(1), pp. 903-939 (2005).
16. BSI-6349-3 "Design of drydocks, locks, spillways, and shipbuilding berths, ship lifts and dock and lock gates", *British Standard Code of Practice for Maritime Structures*, **3**, pp. 20-75 (1988).
17. USACE "Unified Facilities Criteria (UFC), design of graving docks", *Tech. Report No. 4-213-10 Submitted to USACE*, USA, pp. 50-104 (2002).

BIOGRAPHIES

Ataollah Najafi Jilani is Assistant Professor in the Faculty of Civil Engineering in Tarbiat Modares University, Tehran, Iran. He earned his BS degree in Civil

Engineering in 1995 from Tehran Polytechnic (Amir-Kabir) University of Technology, his MS degree in Hydraulic Structures Engineering in 1997 from Tehran University, and his PhD in Civil-Hydraulic Engineering in 2007 from Sharif University of Technology, Tehran, Iran.

His major award is the 22nd Khawrizmi International Award (2009) for third ranking in applicable researchers in Iran entitled "Landslide Generated Waves in Dam Reservoirs". He was the first co-author of this project. He was also in the first ranking of graduated PhD students in the Civil Engineering Department of Sharif University of Technology, and earned the Tavakkoli Prize for the Civil Engineering Department in 2009. He was also in the first rank of graduated MS students earning a graduation ceremony award at the University of Tehran (1997).

Dr. Najafi-Jilani has written 8 journal papers and more than 25 national and international conference papers. The main topics of his research interests are: Numerical and Experimental Investigations on Hydraulic Engineering, Coastal Hydrodynamics, Marine Structures and Coastal Sedimentation.

Morteza Monshizadeh is senior researcher at the Water Research Institute of the Ministry of Power in Iran. He earned his BS degree in Mechanical Engineering in 1991 from K.N.T University of Technology and a MS degree in Energy Engineering in 1995 from the Department of Science and Research of the Islamic Azad University. He was selected in the first rank of researchers in the Ministry of Power in 2001. Mr. Monshizadeh has written 5 journal papers and more than 15 conference papers. His main research interests are: Coastal Engineering, Coastal Sedimentation and Marine Structures.

Abbas Naghavi is presently a MS student in the Civil Engineering department of Tarbiat Modares University, Tehran, Iran. The main topic of his MS Thesis is: "Investigation of the Seawater Flow Pattern Through Flooding Systems and Sea-Structure Interaction". He earned his BS degree in 2006 from the Gorgan Branch of the Islamic Azad University in Tehran, Iran.